Journal of Marine Science and Application (2019) 18:247–259
https://doi.org/10.1007/s11804-019-00101-w

RESEARCH ARTICLE

Analysis of Ocean Wave Characteristic Distributions Modeled by Two Different Transformed Functions

Duanfeng Han[1] · Ting Cui[1] · Yingfei Zan[1] · Lihao Yuan[1] · Song Ding[2] · Zhigang Li[3]

Received: 26 March 2018 / Accepted: 21 January 2019 / Published online: 6 August 2019

Abstract
The probability distributions of wave characteristics from three groups of sampled ocean data with different significant wave heights have been analyzed using two transformation functions estimated by non-parametric and parametric methods. The marginal wave characteristic distribution and the joint density of wave properties have been calculated using the two transformations, with the results and accuracy of both transformations presented here. The two transformations deviate slightly between each other for the calculation of the crest and trough height marginal wave distributions, as well as the joint densities of wave amplitude with other wave properties. The transformation methods for the calculation of the wave crest and trough height distributions are shown to provide good agreement with real ocean data. Our work will help in the determination of the most appropriate transformation procedure for the prediction of extreme values.

Keywords Wave characteristic distributions · Transformed Gaussian process · Transformed function · Parametric method · Non-parametric method · Crossing-density function

1 Introduction

While the probability distribution for stochastic wave characteristics is generally modeled by a Gaussian process using existing methods (Lindgren and Rychlik 1982), the results, especially for the distribution of the crests and troughs, deviate from observations (Ochi and Ahn 1994). Therefore, an appropriate model is needed to analyze the properties of waves. For example, the Slepian model and the regression method may be used to obtain accurate approximations of the distributions of wave characteristics (Lindgren and Rychlik 1991). However, the results derived using a regression-approximation method are often referred to as a "theoretical distribution," since the results differ from the mathematical method, which gives smaller numerical errors. While the distributions proposed by Longuet-Higgins, Cavanie et al. agree well with the theoretical distribution for a narrow-band Gaussian model, these distributions are only based on a few spectral moments, with the agreement with observations worsening for broader spectra (Cavanie et al. 1976). Rychlik and Johannesson analyzed the wave characteristics using the transformed Gaussian model and demonstrated an improved distribution of the wave characteristics with respect to the other models mentioned (Rychlik et al. 1997). However, the transformed Gaussian model lacks an analysis of the transformation function as used by other methods, and it is not clear whether this transformation is able to capture the influence of the distribution of wave characteristics.

Ways to estimate the transformation include that proposed by Ochi and Ahn (1994), which is a monotonic exponential function, while Winterstein's model (Winterstein 1988) is a

Article Highlights
- The real-time wave data of south sea were analyzed by two transformed functions.
- The distribution of wave characteristics had been calculated and the extreme value of wave data had been performed.
- Three different sea states had been analyzed and the best transformed function for each state had been summarized.

Funding item: Supported by the Marine Engineering Equipment Scientific Research Project of Ministry of Industry and Information Technology of PRC and the National Science and Technology Major Project of China (Grant No. 2016ZX05057020) and National Natural Science Foundation of China (Grant No. 51809067)

✉ Yingfei Zan
zanyingfei@hrbeu.edu.cn

[1] College of Shipbuilding Engineering, Harbin Engineering University, Harbin 150001, China

[2] China Ship Research and Development Academy, Beijing 100192, China

[3] Offshore Oil Engineering Co., Ltd., Tianjin 300451, China

monotonic cubic Hermite polynomial, with both transformations using moments to estimate the transformation function g. The Winterstein–Hermite and Ochi models are generally used for the analysis of non-linear vibration problems, such as extreme-value and fatigue analyses, but are rarely used to analyze wave characteristics. In Jean-Marc and Sebastien et al. (Azas et al. 2011), an exact solution for the Hermite method was proposed, but which only gives the extreme behavior of wave models while ignoring the wave characteristic distribution. Rychlik's non-parametric method is based on the crossing intensity (Aberg 2007) for the analysis of the wave distribution to prove the transformed Gaussian model, but lacks a comparison of the different transformations estimated by different methods used in the analysis of wave characteristics. For more exact approximations of the distribution of wave characteristics, and predicting the extreme values, it is essential to analyze the transformed function as estimated by each method.

The analysis of the wave characteristic distribution of the China Sea is in an attempt to provide references for the wave energy resource development, navigation, marine engineering, disaster prevention, and reduction. In China, the wave study mostly based on very limited buoy material or shipping data, so an exact model for wave characteristic analysis is necessary (Zheng et al. 2014). This paper is to compare two methods to choose an appropriately sophisticated one to modeling wave data for evaluation of extreme values.

This paper summarizes two main methods, the parametric and non-parametric methods, to estimate the transformation in transformed Gaussian models. Based on three ocean datasets (Yang et al. 2015) with different significant wave height H_s, two different transformation functions are used here to analyze the probability distribution parameters of wave statistics. First, two transformed functions are obtained using both parametric and non-parametric methods, which are then compared with the empirical distribution of observed wave characteristics. Under the two transformations and combined with the Lindgren distribution, the parameters defining the probability density function for this region are obtained. From these results, the influence of the two different transformations are analyzed for waves with different significant wave heights, and the distributions obtained by the two transformations are compared with determine which gives a better transformation for the analysis of the distributions of wave characteristics.

2 Methodology and Data

The elevation of the sea $X(t)$ as a function of time, sampled at a fixed location, can be written as a function of a Gaussian process $Z(t)$,

$$X(t) = G[Z(t)] \tag{1}$$

where G is a continuously differentiable deterministic function with positive derivatives and $Z(t)$ is a simple stationary Gaussian process with zero mean and a variance of one.

We denote the spectrum of X by $S(w)$, and the spectrum of Z by $\tilde{S}(w)$. The transformation G performs the appropriate non-linear translation and scaling, so that Z is always normalized to have zero mean and a variance of one, and the first spectral moment of Z is one. The calculation uses the inverse function of G, g to define the transformation instead of G, as well as the relation $Z(t) = g\,[X(t)]$ between the observational data $X(t)$ and the transformed data $Z(t)$.

Here, the simplest alternative is used to estimate the function g directly from the data by the following two methods: parametric and non-parametric methods.

2.1 Data

For the analysis of two different transformation functions for waves with different significant wave height H_s, the data adopted in this paper were provided by South China Sea Institute of Oceanography, and three datasets were sampled (Zeng 2015) in the South China Sea (Yang et al. 2015). The analyses of each dataset for two different transformations are presented here. The abbreviation MWL of the Y-axis means "mean water level" in Fig. 1.

Some simple statistics for the observations are given in Table 1, including the sampling interval T_s, the total time of the measurement T, and the significant wave height H_s. For calculating the significant wave height, all turning points had been included in the calculating process.

We define the wave characteristics as shown in Fig. 2.

2.2 Methods

2.2.1 Non-parametric Method

Based on the non-parametric method, the transformed function is calculated using the crossing-density function $V(u)$, which yields the average number, per time or space unit, of up-crossings of the level u. The basic definition of the crossing function is

$$V(u) = E[\text{numbers of up}-\text{crossings of level } u \text{ by } X(t)] \tag{2}$$

where E is the expected value, and V is approximated as

$$V(u) = \frac{1}{T}\sum_i l_{(m_i,M_i]}(u) = \hat{V}(u) \tag{3}$$

where $l_{(m_i,M_i]}(u) = 1$ if $\min < u < \max$ and zero if u out of this range, the min and the max is the local extreme of the wave in index, u is a variable of different levels for the crossing-density function and the transformed function in the next section, by definition of the empirical up-crossing density observed at time

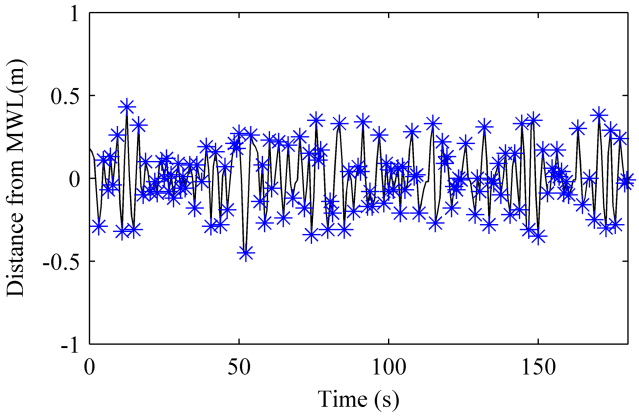

(a) $H_s = 0.54$ m

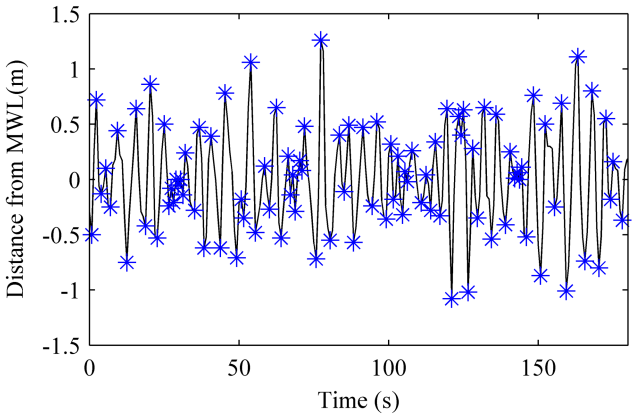

(b) $Hs = 1.67$ m

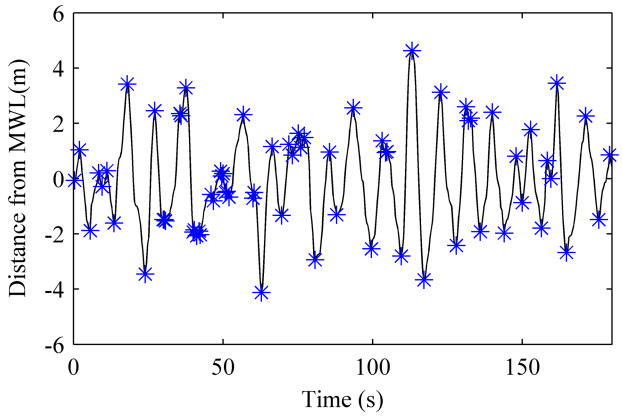

(c) $H_s = 5.32$ m

Fig. 1 Samples of observations with the turning points marked. **a** $H_s = 0.54$m. **b** $H_s = 1.67$m. **c** $H_s = 5.32$m

T, and $\hat{V}(u)$ is not a continuous function. While $V(u)$ is a differentiable function, so the definition of the $\hat{V}(u)$ is modified into a left continuous function as formula 3.

For a zero-mean Gaussian process $Z(t)$, the crossing density $\tilde{V}(u)$ is given by Rice's formula as

$$\frac{\tilde{V}(u)}{V_o} = \frac{\sigma_z}{\sigma_x}\exp\left(-\frac{u^2}{2\sigma_{\tilde{x}}^2}\right) \tag{4}$$

where V_o is the maximum of $\tilde{V}(u)$, and the observed data $X(t)$ are normalized, so that the maximum of the crossing intensity is $(2\pi)^{-1}$. If σ_z^2 and σ_x^2 are the variance of $X(t)$ and $Z(t)$, assuming $\sigma_x^2 = \sigma_z^2 = 1$, then the formula follows

$$\tilde{V}(u) = \frac{1}{2\pi}\exp\left(-\frac{u^2}{2}\right) \tag{5}$$

The empirical crossing intensity $\hat{V}(u)$ calculated from sampled sea data is used to estimate the function $g = G^{-1}$, which can then be used to match the transformed model. For the transformed model $X(t) = G[Z(t)]$, the crossing intensity is

$$V(u) = \tilde{V}[g(u)] = \frac{1}{2\pi}\exp\left(-\frac{g(u)^2}{2}\right) \tag{6}$$

Assuming that $V(u)$ is a continuous and unimodal function with a maximum $u = u_0$, the transformation g is expressed as

$$g(u) = \begin{cases} \sqrt{-2\ln(2\pi V(u))} & \text{if } u \geq u_0 \\ -\sqrt{-2\ln(2\pi V(u))} & \text{if } u < u_0 \end{cases} \tag{7}$$

Since $V(u)$ can be estimated from the data and denoted by the empirical crossing $\hat{V}(u)$, the renormalized empirical transformation function is

$$g^*(u) = \begin{cases} \sqrt{-2\ln(2\pi V(\sigma u + m))} \\ -\sqrt{-2\ln(2\pi V(\sigma u + m))} \end{cases} \tag{8}$$

Since $\hat{V}(u)$ is not a continuous function, then $g^*(u)$ is also not continuous, and hence must be smoothed for the Gaussian process

$$g^s(u) = \begin{cases} \sqrt{[-2\ln(2\pi V(\sigma u + m))] - [-2\ln(2\pi V(\sigma u_0 + m))]} \\ -\sqrt{[-2\ln(2\pi V(\sigma u + m))] - [-2\ln(2\pi V(\sigma u_0 + m))]} \end{cases} \tag{9}$$

which gives the smoothed approximation $g^s(u)$ to $g(\sigma u + m)$. Finally, the estimation of the transformation is

$$g(u) \approx g^s\left(\frac{u-m}{\sigma}\right) \tag{10}$$

So that if $g^s(u) = u$, the Gaussian model for the observational data $X(t)$ can be obtained.

Table 1 Summary of observation statistics

Dataset	Sampling interval T_s (s)	Total sampling time T (s)	Significant wave height H_s (m)
Group 1	0.35	10 883	0.54
Group 2	0.35	10 880	1.67
Group 3	0.78	9880	5.32

2.2.2 Parameter Method

In contrast to the non-parametric method, the function g is estimated by establishing the Hermite polynomial for the parametric method. This section summarizes the transformation function for the analysis of wave characteristics by revisiting the Hermite moment model used to analyze non-linear responses. The transformation uses the moment of $X(t)$ to compute g.

Firstly, $X(t)$ must be normalized by the mean and variance

$$\frac{X-m}{\sigma} = X_0 = G(Z) \tag{11}$$

where m is the mean of $X(t)$, σ is the variance of $X(t)$, and Z is a Gaussian process.

Given N response moments of the process, the transformation for a standardized process is taken as an N-term Hermite series,

$$X_0 = G(Z) = k\left[Z + \sum_{n=3}^{N} \tilde{h}_n He_{n-1}(Z)\right] \tag{12}$$

where $k = 1$ and the wave non-linearity is sufficient, which enables here $\tilde{h}_n$ to be equal to the Hermite moment h_n, $\tilde{h}_n = h_n$. The Hermite moment is related to the central moment α, where α is estimated from the X process,

$$h_n = \frac{\alpha_n}{n!} - \frac{\alpha_{n-2}}{1!2(n-2)} + \frac{\alpha_{n-4}}{2!2^2(n-4)!} - \cdots \tag{13}$$

where

$$\alpha_n = E\left[X_0^n(t)\right] \tag{14}$$

The Hermite polynomials $He_{n-1}(z)$ in particular are

$$\begin{cases} He_1(z) = z \\ He_2(z) = z^2 - 1 \\ He_3(z) = z^3 - 3z \\ He_4(z) = z^4 - 6z^2 + 3 \end{cases} \tag{15}$$

Here, the data are estimated using the central moments $\alpha_4 < 3$, so the Hermite series can be applied to model the transformation to a Gaussian process $Z(t)$ according to

$$g(x) = x_0 - \sum_{n=3}^{N} h_n He_{n-1}(x_0) \tag{16}$$

From Eq. (15), the function g is calculated from the Hermite moment as estimated from the data.

The Hermite series in Eq. (12) is assumed to be monotonic, where the probability distribution function follows from the Gaussian process

$$F_X(x) = P[X(t) \le x] = \Phi[z] \tag{17}$$

where F and Φ are the cumulative functions of $X(t)$ and $Z(t)$, respectively.

3 Theoretical Probability Distribution of Wave Characteristics

For the transformed Gaussian process $Z(t)$, the marginal distribution is approximated accurately using the regression method for Lindgren and Rychlik's distribution (Lindgren et al. 1998; Schuster 1898).

Here this section gives a brief description of the theoretical distribution known as Lindgren and Rychlik's distribution, which requires numerical integration. The Lindgren method consists of using a "model process" to investigate the behavior of the surface near a local maximum (crest) of a given height from which it is possible to estimate the joint distribution of height and period conditional on the value of the crest height. By integrating this distribution over all possible crest heights, the joint distribution of wave height and period is obtained, with the result shown by Srokoze and Challenor (Srokosz and Challenor 1987) to be an adequate approximation; therefore, Lindgren and Rychlik's distribution is called the "regression method."

The marginal distributions of the crest period T_C, trough period T_T crest height A_C and trough height A_T, as well as the joint density of wave characteristics, are approximated by the regression method presented in the next section.

The special joint density of the trough and crest height f_{mM} is used based on Longuet-Higgins's method (Longuet-Higgins 1975; 1983), with the transformation g assumed to be known. The joint probability of the trough and crest is expressed as

$$P(a,b) = P(m < a < b < M) \tag{18}$$

where a, b are fixed levels, u is the reference level for $a < u < b$, and m and M are the heights of the wave troughs and crests, respectively.

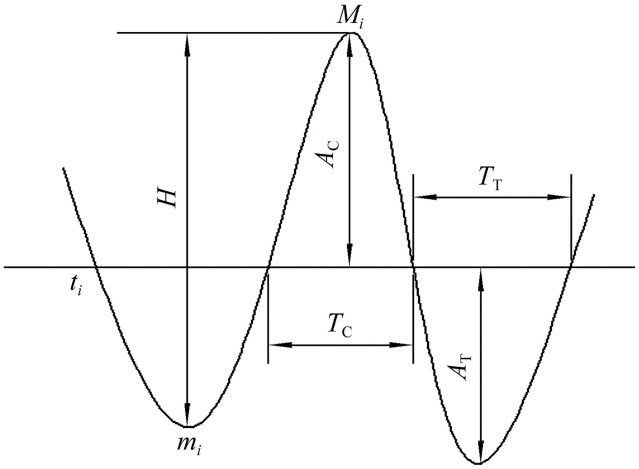

Fig. 2 Definition of wave characteristics

The joint density is calculated as

$$f_{mM}(a,b) = -\frac{\partial^2 P(a,b)}{\partial a \partial b} \tag{19}$$

for which the approximate definition of $P(a, b)$ is defined by the "Palm distribution" simply as the proportion of waves for which $m < a < b < M$ according to

$$P(a,b) = \lim_{\tau\to\infty} \frac{\mathrm{Num}\{t_i \in [0,\tau] : m_i < a < b < M_i\}}{\mathrm{Num}\{t_i \in [0,\tau]\}} = \frac{\text{intensity of trough} < u \text{ and crest} > v}{\text{intensity of waves}} \tag{20}$$

where Num is the number of elements in the set{}, X is the observed data, t_i is the up-crossing time of the reference level u, and m_i and M_i are the trough and crest heights of each wave, respectively. Further details concerning this expression are found in Rychlik et al. (1995).

4 Calculated Transformations

The calculation of level u-up-crossing (level crossing density) is to estimate the transformed function of the parametric method in transformation and then in parametric method, the wave characteristics of transformed Gaussian process could be analyzed. Before calculating the transformation g by the non-parametric method, the crossing density is estimated from the three datasets for the crossing intensities shown in Fig. 2.

The transformations are estimated for the three datasets, indicating distributions with a light lower tail and heavy upper tail compared with a Gaussian model. For comparison of the transformed functions, Fig. 3 shows the results produced by unsmoothed transformations g^* estimated by the non-parametric method according to Eq. (8) as well as the transformation g_{lc} that uses Eq. (10), which is a smoothed transformation estimated by the non-parametric method. The abbreviation g_h represents a transformation estimated by the parametric method (see Eq. (16)). These transformations are compared with the linear transformation $g(u) = u$, which represents the Gaussian process and use g_u represents $g(u) = u$.

From Fig. 4, all transformations deviate from the straight line $g = (u)$ representing the Gaussian model, as well as from each other, and two of the transformations g_{lc} and g_h overestimate the crest height and underestimate the lower trough. Comparing the two transformations g_{lc} and g_h for the lowest significant wave height, g_{lc} deviates only slightly from g_h, with g_h giving slightly higher crests than g_{lc} when the crest height exceeds H_s. As H_s increases, the g_h transformation deviates from the g_{lc} transformation for $u > 1.2$, which also means the g_{lc} transformation gives higher crests in the case that the wave height exceeds H_s. However, with regard to troughs, the two transformations do not deviate greatly from each other in the second dataset. In the dataset with the highest H_s, the g_h and g_{lc} transformations exhibit reverse behavior, with the g_{lc} transformation giving a higher crest, but with g_h giving a lower trough than g_{lc}. However, from Fig. 3, it can be seen that the different influences on the wave characteristics need to be analyzed in detail by two transformations, as performed in the next section.

Although the deviation of the two transformations from a Gaussian process may be clear, the degree to which this occurs should be quantified. The function $e(g)$ used as a test quantity for the non-Gaussian nature of the data was transformed by the different transformation function g, with the value of $e(g)$ giving a measure of the deviation of g from a Gaussian model. The departure of each transformation function from the Gaussian process is calculated by $e(g)$, which is defined as

$$e(g) = \left(\int_{-\infty}^{\infty} (g(u)-u)^2 \mathrm{d}u\right)^{1/2} \tag{21}$$

For an ergodic Gaussian process, and from the definition of $e(g)$, the value of $e(g)$ is zero if the number of the sampled data amounts to an infinite process. The results are calculated for 100 sampled data points as shown in Fig. 4, where the dash–dotted line is the test value of the transformation g_h and the dashed line is the result of g_{lc} (Fig. 5).

From Fig. 4, the data depart from a Gaussian process significantly, and the testing value of two transformations all deviate from the Gaussian process as summarized in Table 2. The green dots represent the department between observed data and Gaussian process.

As the values of the two transformations are different from each other, the transformed process $X(t)$ may also be different, so the analysis of the resulting wave characteristics becomes essential, particularly the extent to which different functions alter the distributions.

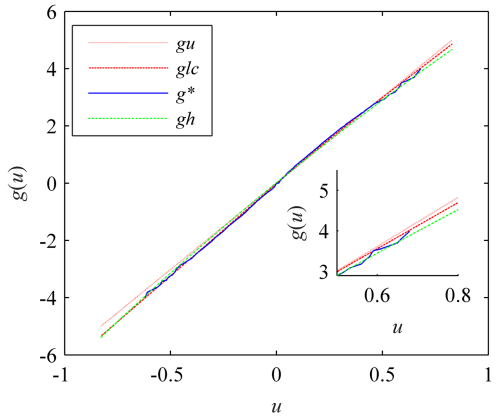

(a) H_s = 0.54 m

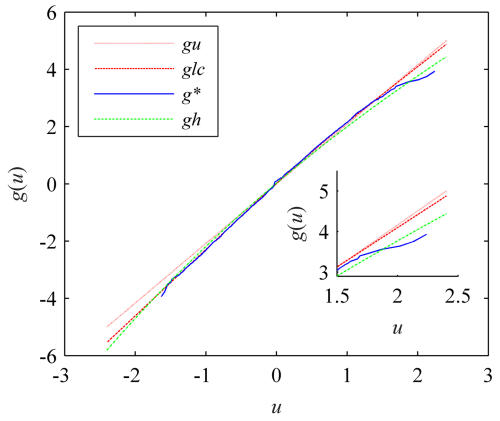

(b) H_s = 1.67 m

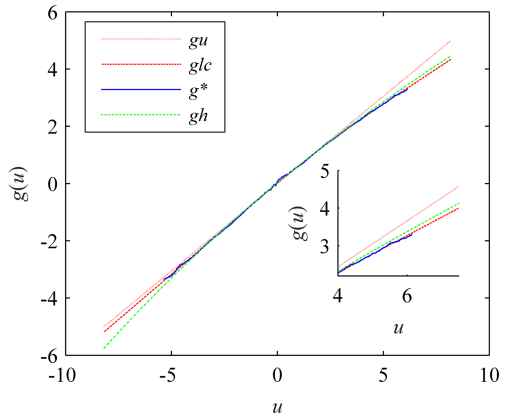

(c) H_s = 5.32 m

Fig. 3 The crossing intensity of observations compared with theoretical Gaussian distributions. **a** H_s = 0.54m. **b** H_s = 1.67m. **c** H_s = 5.32m

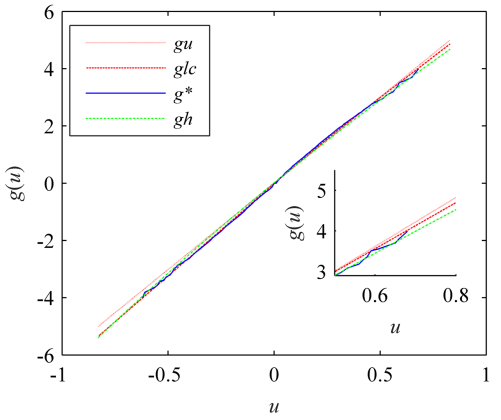

(a) H_s = 0.54 m

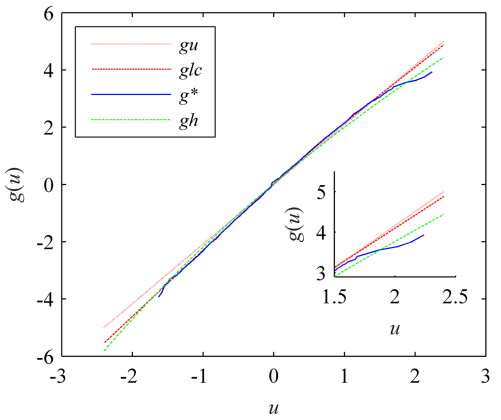

(b) H_s = 1.67 m

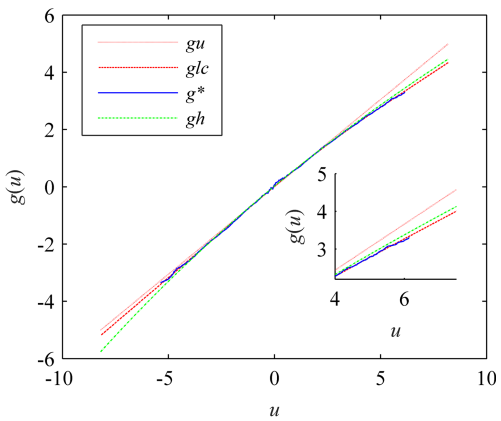

(c) H_s = 5.32 m

Fig. 4 Comparison of the four transformations g for different values of H_s. **a** H_s = 0.54m. **b** H_s = 1.67m. **c** H_s = 5.32m

The next important parameter in estimating the transformed Gaussian model is the spectra $S(w)$, which is simulated using the correlation function algorithm.

The spectral density function S of two datasets estimated with two different transformations is shown in Fig. 6, with the dashed line illustrating the transformation g_{lc} and the solid line the transformation g_h.

5 Results and Discussion

The distributions of the wave properties presented here were calculated with the help of the WAFO toolbox (Rychlik and Lindgren 2011). The method of observed data and transformed process's distribution analysis were the same

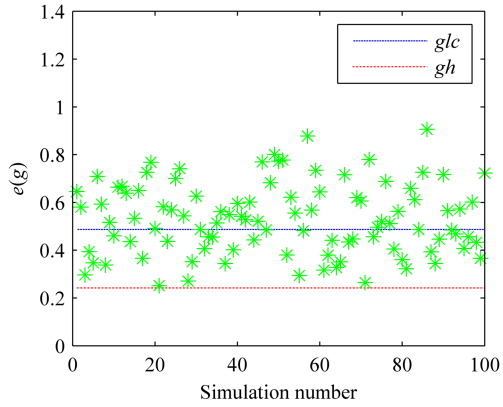

(a) $H_s = 0.54$ m

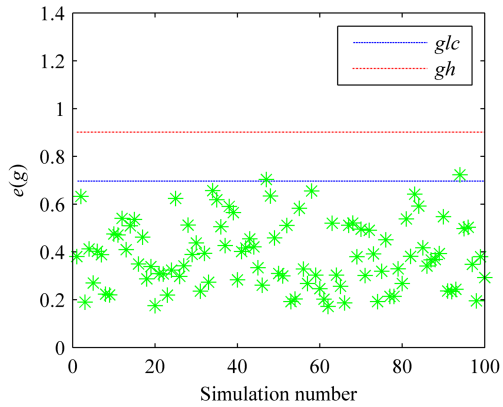

(b) $H_s = 1.67$ m

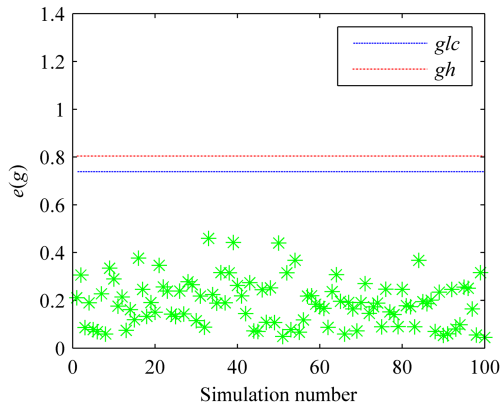

(c) $H_s = 5.32$ m

Fig. 5 Comparison of the function $e(g)$ for the four transformations g with different values of H_s. **a** $H_s = 0.54$m. **b** $H_s = 1.67$m. **c** $H_s = 5.32$m

one, so the difference between different transformations and observed means the error.

Table 2 Values of $e(g)$ of two transformations with different values of H_s

H_s (m)	0.54	1.67	5.32
$e(g_{lc})$	0.4871	0.6967	0.7384
$e(g_h)$	0.2424	0.9014	0.8038

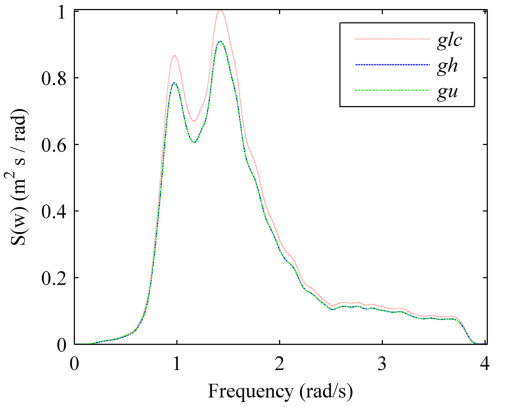

(a) $H_s = 0.54$ m

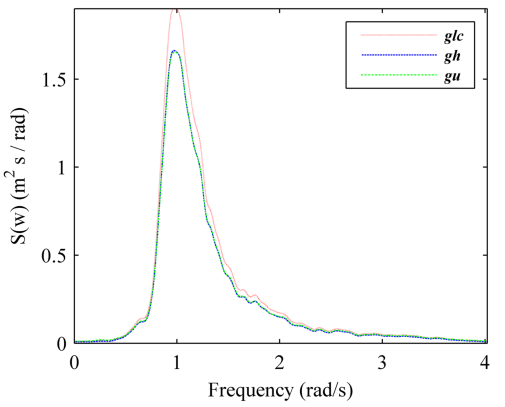

(b) $H_s = 1.67$ m

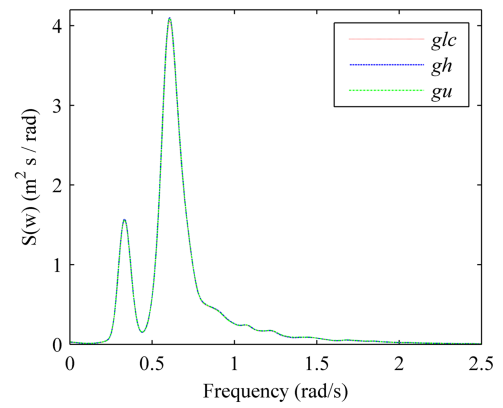

(c) $H_s = 5.32$ m

Fig. 6 Spectra of two different transformation processes. a $H_s = 0.54$m. **b** $H_s = 1.67$m. **c** $H_s = 5.32$m

5.1 Marginal Distribution of Wave Characteristics

The discussion below focuses on analysis of the marginal distribution of wave characteristics. The density values of the crest wave period T_C calculated by two transformations are compared with the empirical distribution estimated from

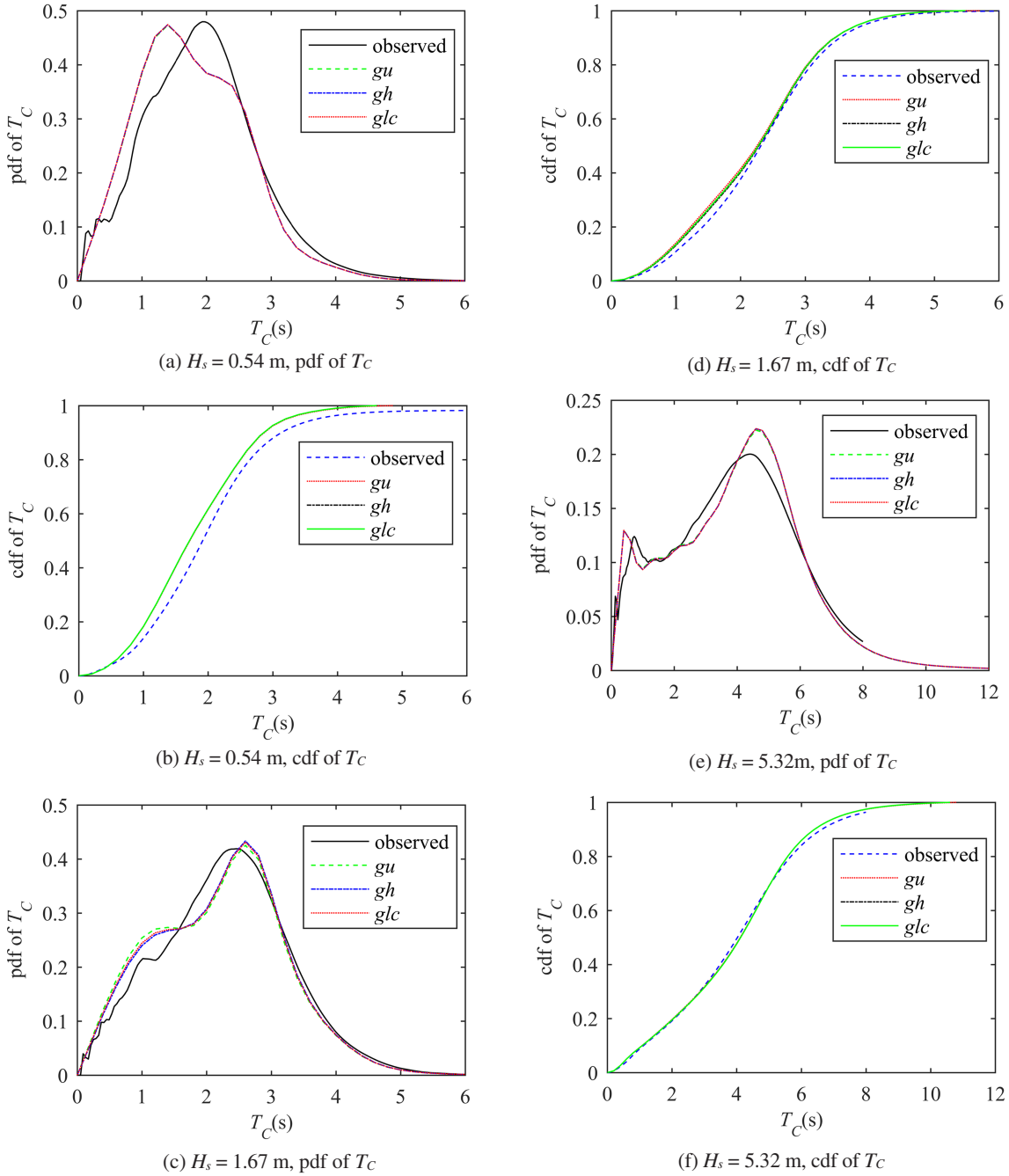

(a) $H_s = 0.54$ m, pdf of T_C

(d) $H_s = 1.67$ m, cdf of T_C

(b) $H_s = 0.54$ m, cdf of T_C

(e) $H_s = 5.32$m, pdf of T_C

(c) $H_s = 1.67$ m, pdf of T_C

(f) $H_s = 5.32$ m, cdf of T_C

Fig. 7 Probability and cumulative density functions for T_C. **a** $H_s = 0.54$m, pdf of T_C. **b** $H_s = 0.54$m, cdf of T_C. **c** $H_s = 1.67$m, pdf of T_C. **d** $H_s = 1.67$m, cdf of T_C. **e** $H_s = 5.32$m, pdf of T_C. **f** $H_s = 5.32$m, cdf of T_C.

the whole observed data, and the probability and cumulative density functions (pdf and cdf, respectively) are calculated and shown in Fig. 7.

For the pdf of T_C, the transformed processes of the g_{lc} and g_h transformations match well with the Gaussian process $g(u) = u$, with the wave period in $X(t)$ equal to that of a Gaussian process. However, the empirical distribution obtained from the data deviates from the others in the range of the extreme value for all H_s because of the T_C probability density as a short wave with a small amplitude around the peaking; however, the numerical integration could have low accuracy for small amplitudes.

The cdf narrowed the gap and all of them have a good agreement, with the results indicating that the wave-period distribution of the two transformations g_{lc} and g_h for processes $G[Z(t)]$ is in agreement with the observations. The small changes in both the crest wave period and crossing density indicate that the calculations are accurate.

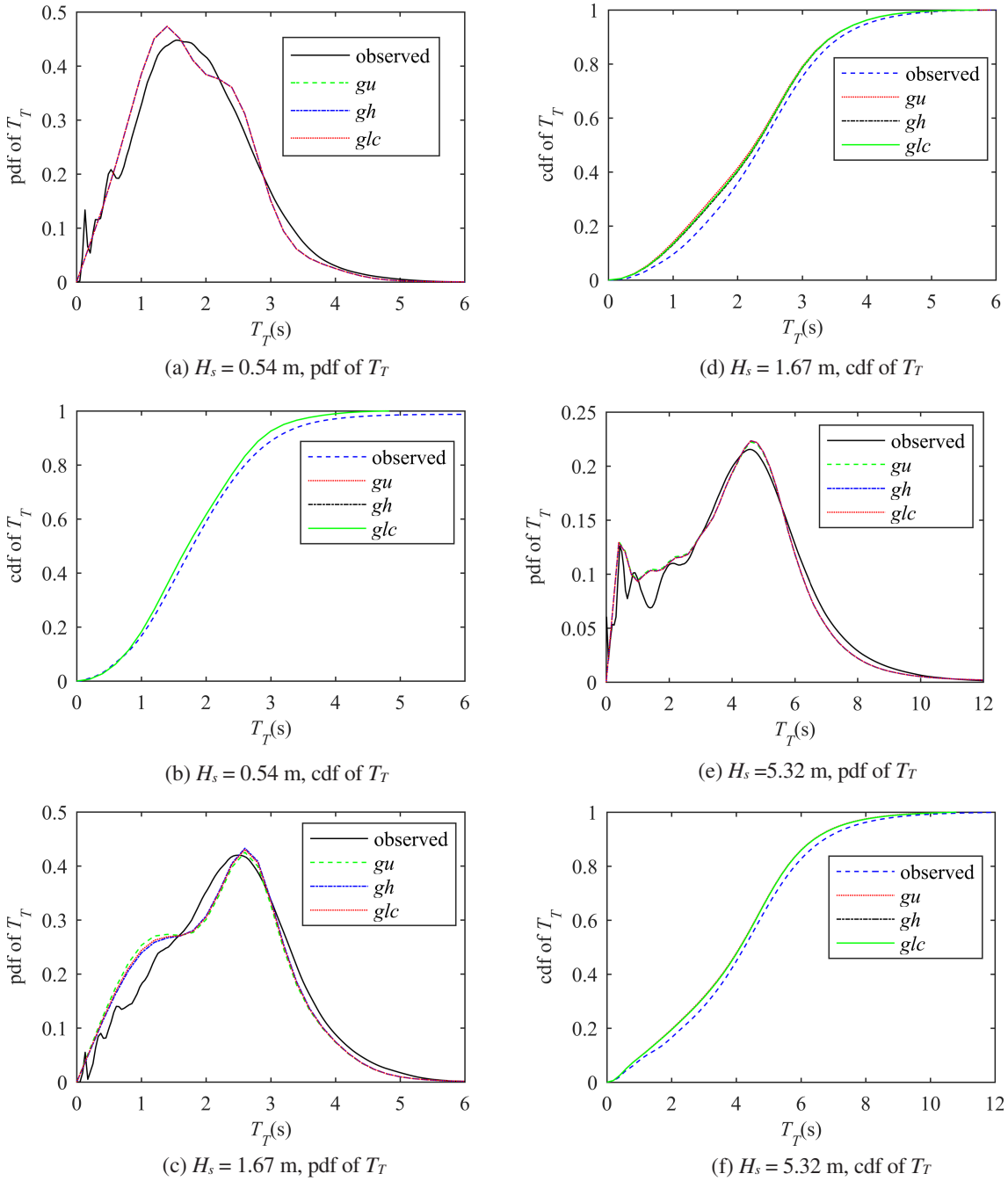

(a) H_s = 0.54 m, pdf of T_T

(d) H_s = 1.67 m, cdf of T_T

(b) H_s = 0.54 m, cdf of T_T

(e) H_s =5.32 m, pdf of T_T

(c) H_s = 1.67 m, pdf of T_T

(f) H_s = 5.32 m, cdf of T_T

Fig. 8 Probability and cumulative distribution functions of T_T. **a** H_s = 0.54m, pdf of T_T. **b** H_s = 0.54m, cdf of T_T. **c** H_s = 1.67m, pdf of T_T. **d** H_s = 1.67m, cdf of T_T. **e** H_s = 5.32m, pdf of T_T. **f** H_s = 5.32m, cdf of T_T.

For the wave trough period T_T, the pdf and cdf are calculated similarly to the crest period T_C, with the results shown in Fig. 8.

The results for the density of the trough period are similar to those of the crest period. From the cdf, the trough period estimated by the two transformations and the Gaussian process also exhibits little deviation from the empirically estimated distributions. Consequently, the results estimated by the transformation for the trough period are accurate, and, with regard to the theoretical crest period, give good agreement for estimation of the minimum. As the maximum and minimum values are estimated accurately, the extreme values may also be estimated accurately regardless of the transformation method employed.

Of interest is the wave amplitude distribution shown in Fig. 9, where the transformation g_{lc} matches well with the observations regardless of the significant wave height. In contrast, for data of lower H_s, the transformation g_h and Gaussian

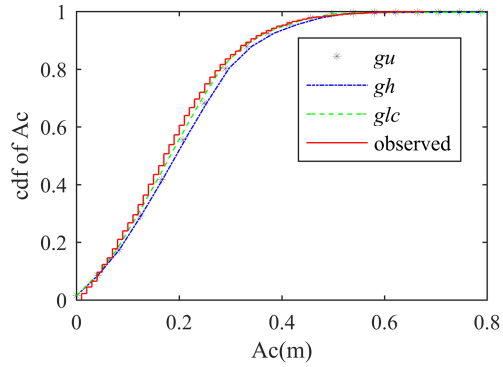

(a) $H_s = 0.54$ m

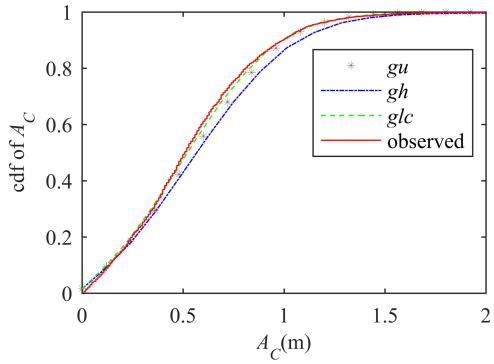

(b) $H_s = 1.67$ m

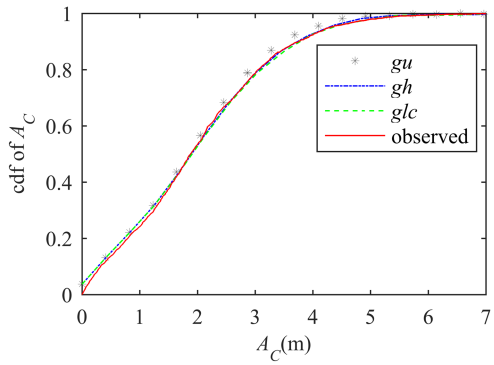

(c) $H_s = 5.32$ m

Fig. 9 Cumulative distribution function of A_C.

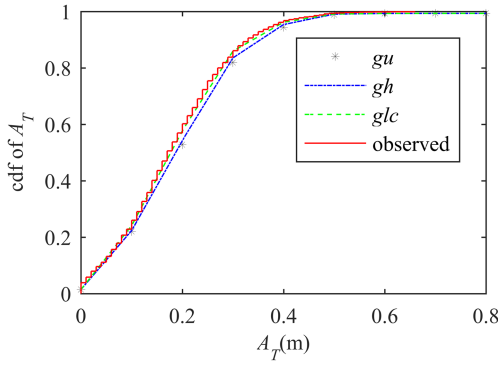

(a) $H_s = 0.54$ m

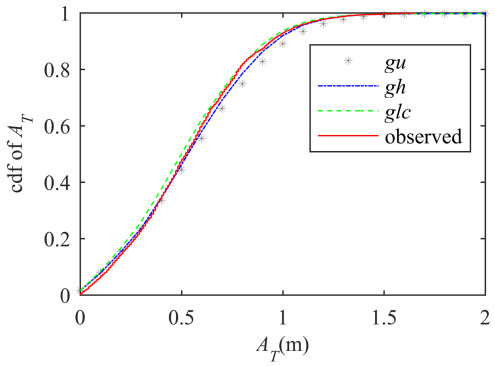

(b) $H_s = 1.67$ m

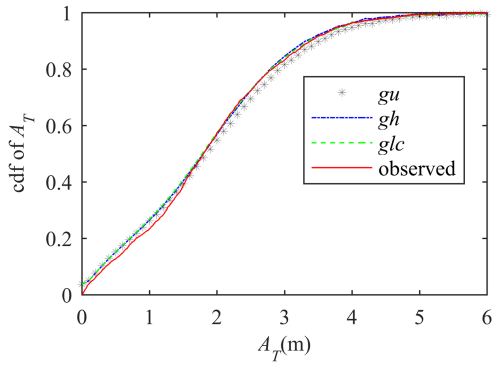

(c) $H_s = 5.32$ m

Fig. 10 Cumulative distribution function of A_T. **a** H_s = 0.54m. **b** H_s = 1.67m. **c** H_s = 5.32m

process $g(u) = u$ deviate from the observations as is evident in Fig. 9(b), but with good agreement again for $H_s = 5.32$ m, as shown in Fig. 9(c). Therefore, while the g_{lc} and g_h transformations as well as the Gaussian process $g(u) = u$ may give equivalent crest heights with higher H_s, the transformation g_{lc} could give better estimates of the crest height with lower significant wave heights.

In Fig. 10, the abscissa represents the absolute value of the true value. The two transformations give results in good agreement with the observed data, meaning that the predicted distribution of the trough height obtained from the two transformations and the Gaussian process yield similar results as the result analysis of crest height. In particular, the two transformed processes deliver identical results for the trough distribution.

5.2 Joint Density of the Wave Characteristics

Wave joint densities were calculated in this part, and the results were estimated from three groups as follows.

The joint densities are displayed in Fig. 11, similar shapes of joint density functions are estimated by the two transformations, but with deviations in the range around the peaks. For $H_s = 0.54$ m and $H_s = 1.67$ m, the transformation g_h attains a higher crest amplitude for the same T_C and includes more dots than the g_{lc} transformation, but a higher amplitude is attained by the g_{lc} transformation for $H_s = 5.32$ m than the g_h transformation for the same T_C.

Figure 12 shows the asymmetric joint distributions as estimated by the two transformations g_{lc} and g_h, with the

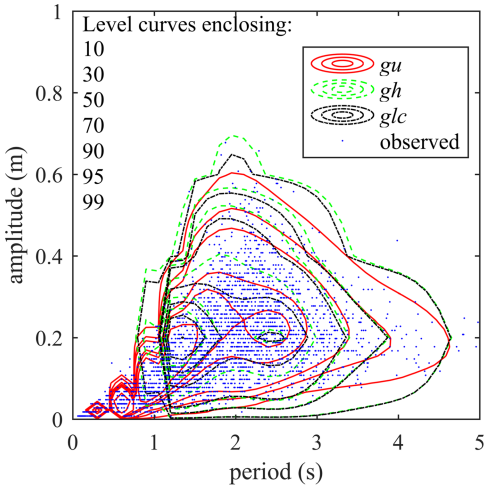

(a) $H_s = 0.54$ m

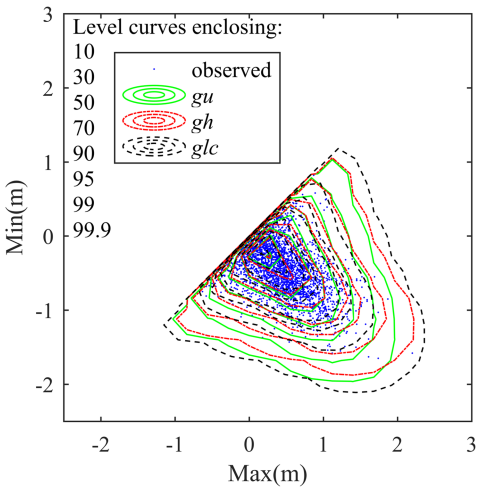

(b) $H_s = 1.67$ m

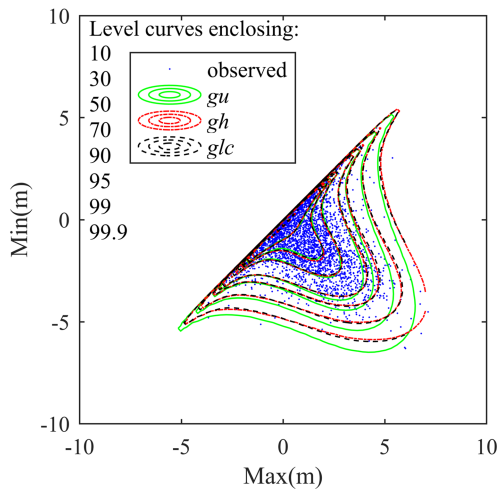

(c) $H_s = 5.32$ m

Fig. 11 Joint density of the crest period and crest amplitude. **a** H_s = 0.54m. **b** H_s = 1.67m. **c** H_s = 5.32m

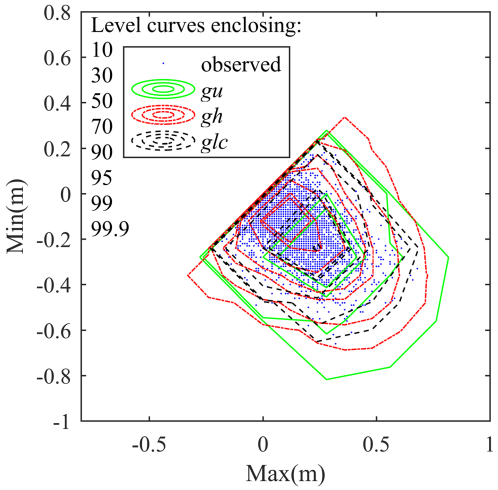

(a) $H_s = 0.54$ m

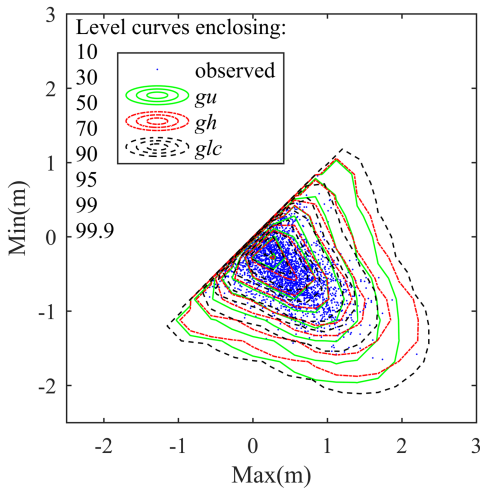

(b) $H_s = 1.67$ m

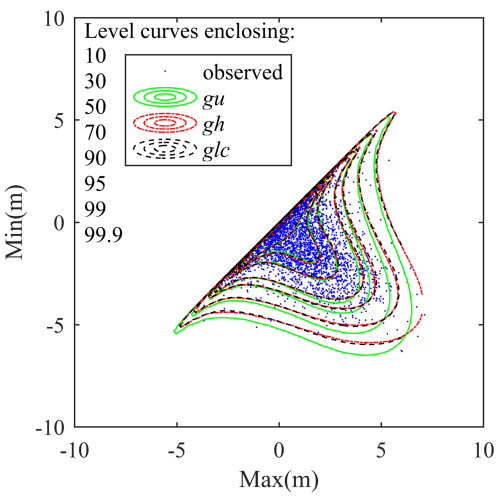

(c) $H_s = 5.32$ m

Fig. 12 Joint density of the maximum and the following minimum wave heights. **a** $H_s = 0.54$ m. **b** $H_s = 1.67$ m. **c** $H_s = 5.32$ m

maximum wave heights being relatively higher than the corresponding minimum values, which is consistent with the observations. For $H_s = 0.54$ m and $H_s = 1.67$ m, the transformation g_h gives better approximations than the g_{lc}

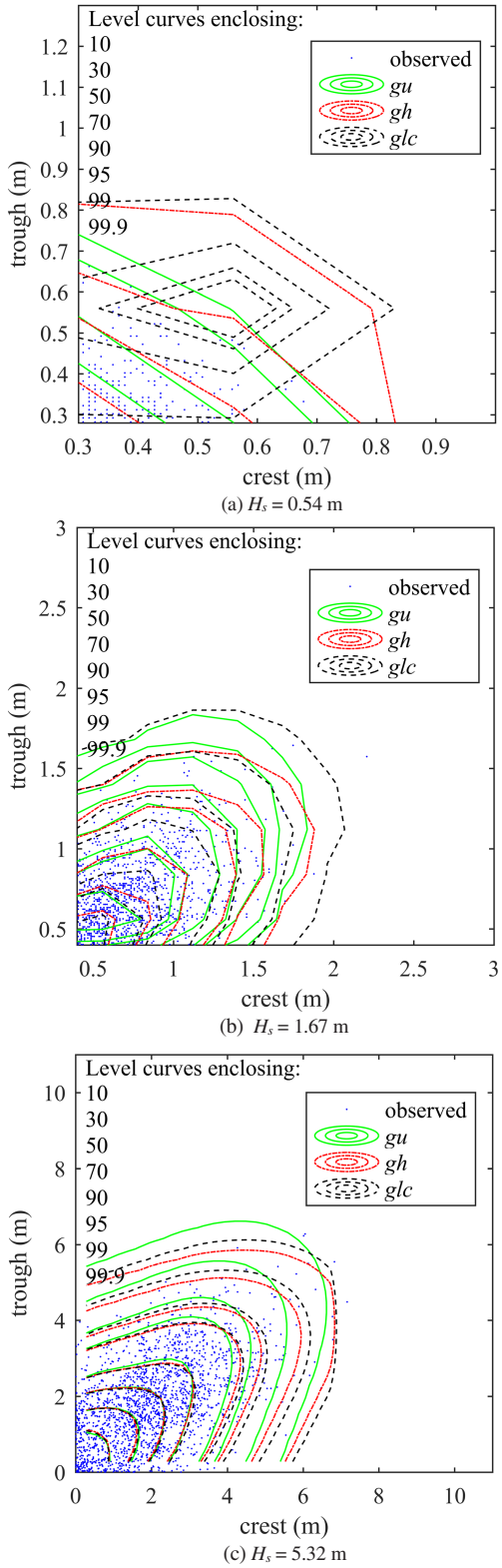

Fig. 13 Joint density of the crest and trough heights. **a** H_s = 0.54m. **b** H_s = 1.67m. **c** H_s = 5.32m

transformation, although in Fig. 12b, the line indicating the estimation from the g_{lc} transformation includes more data points than for the g_h transformation, which may give greater errors than the g_h transformation when predicting the relative heights of the maximum and following minimum wave heights.

The joint density of the trough and crest heights was obtained using the Markov-chain approximation for the sequence of turning points of the three datasets. As for the joint density of the maximum and minimum wave heights shown in Fig. 12, the lines of the transformed process compare well with the observed crests and troughs. From Fig. 13, the function estimated by the g_{lc} transformation gives good agreement with the observations compared with the g_h transformation, resulting in greater crest heights than trough heights.

6 Conclusions

The paper has presented the analysis of two transformation functions g_{lc} and g_h estimated from two different methods for three wave datasets of different H_s, and found differences in the distributions of wave characteristics modeled by the two transformations. For the marginal distribution of wave characteristics, especially for the distributions of A_C and A_T, the transformation g_{lc} gives a better approximation than the g_h transformation independent of the value of H_s. For the T_C and T_T values, the two transformations give good agreement with the observed data, which gives confidence in the accuracy of the calculation of the joint density. For the joint density of A_C and T_C, the transformation g_h gives better approximations than g_{lc} for $H_s < 1.67$ m. As H_s increases, the results estimated by the transformation g_{lc} are superior to that for the g_h transformation. For the joint density of the maximum and minimum heights, as well as the joint density of the crest and trough heights, the transformation g_{lc} gives a better approximation than the g_h transformation independent of the value of H_s. Both transformations could give asymmetric characteristic of the extreme joint distribution. However, the results of the non-parametric transformation were similar to Gaussian process especially for A_C and A_T analysis with the lower H_s. Comparing the non-parametric method, the parametric method could give more accurately the result of the extreme distribution analysis.

Results of distributions imply that the two transformations give more accurate approximations than the Gaussian process, at least for the data considered here. The transformations do not change the crossing density of the observed data, which gives confidence in the values for the crest and trough heights. The difference in the approximations estimated by the two transformations gives different wave characteristics for different H_s. According to results related to the crest and trough heights, the transformation g_{lc} yields a better approximation than the g_h transformation. For the relationship between the wave period and the corresponding amplitude, the transformation g_h produces a better approximation for $H_s < 1.67$ m, but a

higher H_s leads to a superior performance of the g_{lc} transformation.

Above all, the transformation estimated by the parametric method predicts the distributions of wave characteristics more accurately, especially the height of local maxima and wave crest and trough height (A_C, A_T), for Gaussian process gives less non-linear result. The transformed function and the distribution of local extreme values all show the department of the Gaussian process, which should be called the non-Gaussian. These results also express the non-Gaussian behavior of the actual ocean wave data relative to the Gaussian process. This implies that the transformed models would be necessary if the extreme wave characteristic has to be modeled. On the other hand, the marginal distributions of the wave period and amplitude were also modeled well by the Gaussian process. Finally, as the transformed Gaussian model is still too simple to provide more accurate predictions for extreme values, recommending the use of the general class of transformation model is presented here.

References

Aberg S (2007) Application of Rice's formula in oceanographic and environmental problems. PhD thesis, Mathematic Statistical, Center for Mathematics Science, Lund Univiversity, Sweden

Azas J-M, Déjean S, León JR, Zwolska F (2011) Transformed Gaussian stationary models for ocean waves. Probab Eng Mech 26:342–349. https://doi.org/10.1016/j.probengmech.2010.09.007

Baxevani A (2004) Modelling sea surface dynamics using crossing distributions. PhD thesis, Mathematic Statics, Center for Mathematics Science, Lund Univiversity, Sweden

Baxevani A, Rychlik I (2006) Maxima for Gaussian seas. Ocean Eng 33: 895–911. https://doi.org/10.1016/j.oceaneng.2005.06.006

Brodtkorb P, Myrhaug D, Rue H (2001) Joint distribution of wave height and wave crest velocity from reconstructed data with application to ringing. Int J Offshore Polar Eng 11(1):23–32

Buows E, Gunther H, Rosenthal W, Vincent C (1985) Similarity of the wind wave spectrum in finite depth water 1. Spectral form. J Geophys Res 90(C1):975–986. https://doi.org/10.1029/JC090iC01p00975

Cavanie A, Arhan M, Ezraty R (1976) A statistical relationship between individual heights and periods of storm waves. In: Proc. conf. on behavior of offshore structures, Trondheim. Norvegian Institute of Technology, Trondheim, 354–360

Coles S (2001) An introduction to statistical modeling of extreme values. Springer-Verlag, London

Lindgren G (1972) Wave-length and amplitude in Gaussian noise. Adv Appl Probab 4:81–108. https://doi.org/10.1017/S0001867800038179

Lindgren G, Rychlik I (1982) Wave characteristic distributions for Gaussian waves–wave-length, amplitude, and steepness. Ocean Eng 9:411–432. https://doi.org/10.1016/0029-8018(82)90034-8

Lindgren G, Rychlik I (1991) Slepian models and regression approximations in crossing and extreme value theory. Int Stat Rev 59(2):195–225. https://doi.org/10.2307/1403443

Lindgren G, Rychlik I (1993) CROSSING – a technique for first passage and wave density analysis. Probab Eng Inf Sci 7:125–148. https://doi.org/10.1017/S0269964800002825

Lindgren G, Rychlik I, Prevosto M (1998) The relation between wave length and wave period distributions in random Gaussian waves. Int J Offshore Polar Eng 8(4):258–264

Longuet-Higgins (1975) On the joint distribution wave periods and amplitudes of sea waves. J Geophys Res 80:2688–2694. https://doi.org/10.1029/JC080i018p02688

Longuet-Higgins (1983) On the joint distribution of wave periods and amplitudes in random wave field. Proc R Soc A 389:241–258. https://doi.org/10.1098/rspa.1983.0107

Marthinsen T, Winterstein S (1992) On the skewness of random surface waves. Int J Offshore Polar Eng. Conerence, ISOPE, San Francisco, USA, III, 472–478

Ochi M, Ahn K (1994) Probability distribution application to non-Gaussian random process. Probab Eng Mech 9:255–264. https://doi.org/10.1016/0266-8920(94)90017-5

Rychlik I, Lindgren G (2011) Matlab toolbox for analysis of random waves and loads–a tutorial. Statures Research Report, Department of Mathematic Statistical, Lund University

Rychlik I, Lindgren G, Lin YK (1995) Markov based correlations of damages in Gaussian and non-Gaussian loads. Probab Eng Mech 10:103–115. https://doi.org/10.1016/0266-8920(95)00001-F

Rychlik I, Johannesson P, Leadbetter MR (1997) Modelling and statistical analysis of ocean-wave data using transformed Gaussian process. Mar Struct 10:13–47. https://doi.org/10.1016/S0951-8339(96)00017-2

Schuster A (1898) On the investigation of hidden periodicities with application to a supposed 26 day period of meteorological phenomena. Terr Magn Atmos Electr 3:13–41

Srokosz MA, Challenor PG (1987) Joint distributions of wave height and period, a critical comparison. Ocean Eng 14:295–311. https://doi.org/10.1016/0029-8018(87)90029-1

Winterstein S (1988) Nonlinear vibration models for extremes and fatigue. J Eng Mech 114(10):1772–1790. https://doi.org/10.1061/(ASCE)0733-9399(1988)114:10(1772

Yang L, Wang D, Huang J, Wang X, Zeng L, Wang S, Chen R, Yuan J, Wang Q, Chen J, Zu T, Li J (2015) Toward a mesoscale hydrological and marine meteorological observation network in the South China Sea. Bull Am Meteorol 96(7):1117–1135. https://doi.org/10.1175/BAMS-D-14-00159.1

Zeng L, Wang Q, Chen R, Wang D (2015) Hydrographic field investigations in the Northern South China Sea by open cruises during 2004-2013. Sci Bull 60(6):607–615. https://doi.org/10.1007/s11434-015-0733-z

Zheng CW, Zhou L, Jia BK, Pan J, Li X (2014) Wave characteristic analysis and wave energy resource evaluation in the China Sea. J Renew Sust Energ 6:043101. https://doi.org/10.1063/1.4885842